JOURNAL OF BACTERIOLOGY, July 1997, p. 4087–4095 Vol. 179, No. 13
0021-9193/97/$04.00+0

The Helicase Domain of Phage P4 α Protein Overlaps the Specific DNA Binding Domain

GÜNTER ZIEGELIN,[1] RICHARD CALENDAR,[2] RUDI LURZ,[1] AND ERICH LANKA[1]*

Max-Planck-Institut für Molekulare Genetik, Dahlem, D-14195 Berlin, Germany,[1] and Department of Molecular and Cell Biology, University of California, Berkeley, California 94720-3202[2]

Received 9 December 1996/Accepted 19 April 1997

Replication initiation depends on origin recognition, helicase, and primase activities. In phage P4, a second DNA region, the *cis* replication region (*crr*), is also required for replication initiation. The multifunctional α protein of phage P4, which is essential for DNA replication, combines the three aforementioned activities on a single polypeptide chain. Protein domains responsible for the activities were identified by mutagenesis. We show that mutations of residues G506 and K507 are defective in vivo in phage propagation and in unwinding of a forked helicase substrate. This finding indicates that the proposed P loop is essential for helicase activity. Truncations of gene product α (gpα) demonstrated that 142 residues of the C terminus are sufficient for specifically binding *ori* and *crr* DNA. The minimal binding domain retains gpα's ability to induce loop formation between *ori* and *crr*. In vitro and in vivo analysis of short C-terminal truncations indicate that the C terminus is needed for helicase activity as well as for specific DNA binding.

The DNA replication of the temperate satellite phage P4 of *Escherichia coli* is driven by the phage-encoded, multifunctional α protein of 777 amino acid residues (12, 16, 31). This protein has primase and helicase activities, binds DNA specifically, and interacts with the phage-encoded protein Cnr (copy number regulation) (30, 33). Defined domains indicate the modular structure of the α protein (30, 32). The primase domain of gene product α (gpα) is related in sequence to that of primases of conjugative plasmids (27), and one of the essential motifs is present in each of the known prokaryotic priming enzymes (20, 31). The domain for primase, containing the motif -EGYATA-, occupies the N-terminal half of gpα. The DNA binding activity is specific for the 6 and 10 TGTTC ACC repeating octamers of the bidirectional replication origin (*ori*) and the *cis* replication region (*crr*), respectively. The iterons located in *ori* are completely conserved, whereas in *crr*, five of the octamers deviate in one position. The DNA binding domain occupies the C-terminal third of gpα. The primase and DNA binding domains can function independently of one another: the N-terminal truncation containing the primase domain complements a P4 primase-null phage, and it retains primase activity in vitro (32). The primase-defective α protein, which has an E214Q mutation, can still bind DNA specifically. The Cnr protein functions as a negative regulator of P4 replication, and P4 phage does not replicate in cells that overexpress *cnr* (28). Mutants suppressing this phenotype map in the DNA binding domain of gpα residing between amino acid residues 675 and 737. Cnr does not bind to DNA by itself, but it alters the DNA binding properties of gpα.

The helicase activity seems to be marked by the Walker type A nucleotide binding site (NBS) motif in the middle of the protein. gpα has 3′→5′ unwinding polarity. The enzyme prefers substrates with non-base-paired tails, resembling the situation of the replication fork. Except for UTP and dTTP, all common nucleotide (or deoxynucleotide) triphosphates (NTPs) can fuel helicase activity (33). Mutations in the nucleotide binding fold abolish the activity of gpα to support phage DNA replication in vivo (32). To define the helicase domain, in this study we tested the ATPase and helicase activities of gpα in a series of mutants that are altered in the NTP binding motif or at the termini of the protein.

* Corresponding author. Mailing address: Max-Planck-Institut für Molekulare Genetik, Abteilung Lehrach, Ihnestrasse 73, Dahlem, D-14195 Berlin, Germany. Phone: 49-30-8413-1562. Fax: 49-30-8413-1690. E-mail: lanka@mpimg-berlin-dahlem.mpg.de.

MATERIALS AND METHODS

Bacterial strains, plasmids, phages, and media. *E. coli* SCS1 (10) was used to maintain plasmids and to overproduce proteins. *E. coli* XL1-Blue (3) was the host for M13 derivatives. *E. coli* C-2309 [*dnaG3* (P2 *lg*) (2)] and C-2422 [*recA*::Cm(P2 *lg del1*) (27)] served for primase complementation experiments. Plasmids and phages used in this study are listed in Table 1. Media used were as described previously (32).

DNA techniques. Standard techniques for plasmid and M13 DNA isolation and molecular cloning were used (23). For site-directed mutagenesis of the α gene (C35H), the method of Sayers et al. (25) was applied with the following synthetic oligodeoxynucleotide: GCCACAGACCGG**GTG**GGGCTGAT GACGG (the deviation from the wild-type α gene [9] is in boldface). The introduced base changes were verified by sequencing with the dideoxy-chain termination method (24), using T7 DNA polymerase. The mutant α-overexpressing plasmid was constructed as described previously (32).

Construction of 5′ and 3′ truncations of the α gene. Each of the oligonucleotide adapters used (Table 2) was designed to restore the appropriate restriction site and to supply original α codons. The positions of the gpα amino acids encoded by the plasmids described are summarized in Fig. 1. Plasmid pST4Δ1, which is nearly identical to pMS4Δ1, contains the α gene under the translational control of the phage T7 *gene10* Shine-Dalgarno sequence. A 472-bp *Nde*I-*Asc*I fragment was generated by PCR using pMS4Δ1 as the template. This fragment, supplying the 5′-terminal portion of the α gene, was fused with the 3′ portion (1,907-bp *Asc*I-*Bam*HI fragment of pMS4Δ1) and coupled to the phage T7 *gene10* Shine-Dalgarno sequence of pDB17HE prepared with *Nde*I and *Bam*HI. The primers were TTCCCGGGCAT**ATG**AAAATGAACGTAACCGCCACCG (P4 coordinates 6945 to 6969) and CATACAGTGGCACCACAAGGTCACC (P4 coordinates 6468 to 6492) (the start codon of the α gene as part of the *Nde*I site is in boldface). To create pMS4Δ3, the 1,304-bp *Nde*I-*Hin*dIII fragment of pMS4Δ4 was replaced by the 1,679-bp *Msc*I-*Hin*dIII fragment of pMS4Δ1 together with an *Nde*I-*Msc*I adapter (T**ATG**CTCCTTTCTCTGG, CCAGAGAA AGGAG**CA**) to supply the start codon. The start codon of gpα and the respective bases of the complementary strand are shown in boldface. To create pMS4Δ4.2, the 424-bp *Dde*I-*Hin*dIII fragment of pMS4Δ4 was replaced by a *Dde*I-*Hin*dIII adapter supplying the original stop codon of the α gene (TCAG AC**TGA**, AGCT**TCA**GTC). The stop codon and the respective bases of the complementary strand are shown in boldface. To create pMS4Δ4.3, the 776-bp *Nde*I-*Afl*II fragment of pMS4Δ4 was replaced by a *Nde*I-*Afl*II adapter (T**ATG**C CGCAGC, TTAAGCTGCGG**CA**) supplying the start codon. To create pMS4Δ4.5, the 606-bp *Eco*RI-*Hin*dIII fragment of pMS4Δ4.3 was replaced by a 499-bp *Eco*RI-*Hin*dIII fragment generated by PCR using pMS4Δ4.3 as the template. The generated fragment contains the codons 625 to 766 of the α gene preceded by the T7 *gene10* ribosome binding site. The primers used were CAC

TABLE 1. Plasmids and phages used in this study

Plasmid or phage	Description	P4 bp coordinates	Reference or source
Plasmids			
pMS119EH	Cloning vector; pMB1 replicon, P*tac*/*lac*; Ap^r		1
pDB17HE	Cloning vector; pMS119HE Ω[pDB173 *Xba*I-*Bam*HI, 2.4 kb]; P*tac*/*lacI*, T7 *gene10* Shine-Dalgarno sequence; Ap^r		19
pMS4Δ1	pMS119EH Δ[pMS4Δ0.5 *Eco*RI-*Eco*RV, 2,462 bp]	7045–4596	27
pMS4Δ1.40	pMS4Δ1 Δ[*Afl*II-*Hin*dIII, 528 bp]Ω[PCR pMS4Δ4.3, *Afl*II-*Hin*dIII, 440 bp]	7045–4651	This work
pMS4Δ1.41	pMS4Δ1 Δ[*Afl*II-*Hin*dIII, 528 bp]Ω[PCR pMS4Δ4.3, *Afl*II-*Hin*dIII, 431 bp]	7045–4660	This work
pMS4Δ1.5	pMS4Δ1 Δ[*Afl*II-*Hin*dIII, 528 bp]Ω[PCR pMS4Δ4.3, *Afl*II-*Hin*dIII, 419 bp]	7045–4672	This work
pMS4Δ1C35G	pMS4Δ1, α C35G mutation	7045–4596	32
pMS4Δ1C35H	pMS4Δ1 α C35H mutation	7045–4596	This work
pMS4Δ1C57G	pMS4Δ1 α C57G mutation	7045–4596	32
pMS4Δ1G506E	pMS4Δ1 α G506E mutation	7045–4596	32
pMS4Δ1K507A	pMS4Δ1 α K507A mutation	7045–4596	32
pMS4Δ1K507D	pMS4Δ1 α K507D mutation	7045–4596	32
pMS4Δ1K507Q	pMS4Δ1 α K507Q mutation	7045–4596	32
pMS4Δ1K507T	pMS4Δ1 α K507T mutation	7045–4596	32
pMS4Δ2	pMS4Δ1 Δ[*Sma*I-*Bam*HI, 1,257 bp]	7045–5850	27
pMS4Δ3	pMS4Δ4 Δ[*Nde*I-*Hin*dIII, 1304 bp]Ω[*Nde*I-*Msc*I adapter,[a] pMS4Δ1 *Msc*I-*Hin*dIII, 1,679 bp]	6255–4596	This work
pMS4Δ4	pMS119EH Ω[T7 *gene10* Shine-Dalgarno sequence, *Nde*I-*Sma*I adapter,[a] pMS4Δ1, *Sma*I-*Hin*dIII, 1,287 bp]	5862–4596	32
pMS4Δ4.2	pMS4Δ4 Δ[*Dde*I-*Hin*dIII, 424 bp]Ω[*Dde*I-*Hin*dIII adapter[a]]	5862–4981	32
pMS4Δ4.3	pMS4Δ4 Δ[*Nde*I-*Afl*II, 776 bp]Ω[*Nde*I-*Afl*II adapter[a]]	5097–4596	This work
pMS4Δ4.5	pMS4Δ4.3 [*Eco*RI-*Hin*dIII, 606 bp]Ω[PCR pMS4Δ4.3, *Eco*RI-*Hin*dIII, 499 bp]	5097–4672	This work
pMS4Δ1thC35G	pMS4Δ1th Δ[*Nde*I-*Asc*I, 472 bp]Ω[PCR pMS4Δ1C35G, *Nde*I-*Asc*I, 472 bp]	7045–4596	This work
pMS4Δ1thC35H	pMS4Δ1th Δ[*Nde*I-*Asc*I, 472 bp]Ω[PCR pMS4Δ1C35H, *Nde*I-*Asc*I, 472 bp]	7045–4596	This work
pMS4Δ1thC57G	pMS4Δ1th Δ[*Nde*I-*Asc*I, 472 bp]Ω[PCR pMS4Δ1C57G, *Nde*I-*Asc*I, 472 bp]	7045–4596	This work
pMS4Δ1thG506E	pMS4Δ1th Δ[*Dra*III-*Afl*II, 560 bp]Ω[pMS4Δ1G506E, *Dra*III-*Afl*II, 560 bp]	7045–4596	This work
pMS4Δ1thK507A	pMS4Δ1th Δ[*Dra*III-*Afl*II, 560 bp]Ω[pMS4Δ1K507A, *Dra*III-*Afl*II, 560 bp]	7045–4596	This work
pMS4Δ1thK507D	pMS4Δ1th Δ[*Dra*III-*Afl*II, 560 bp]Ω[pMS4Δ1 K507D, *Dra*III-*Afl*II, 560 bp]	7045–4596	This work
pMS4Δ1thK507Q	pMS4Δ1th Δ[*Dra*III-*Afl*II, 560 bp]Ω[pMS4Δ1 K507Q, *Dra*III-*Afl*II, 560 bp]	7045–4596	This work
pMS4Δ1thK507T	pMS4Δ1th Δ[*Dra*III-*Afl*II, 560 bp]Ω[pMS4Δ1 K507T, *Dra*III-*Afl*II, 560 bp]	7045–4596	This work
pMS4Δ1th	pST4Δ1 Ω[pTZ1106His *Nde*I-*Nde*I, 368 bp]	7045–4596	This work
pMS4Δ1.5th	pMS4Δ1th Δ[*Afl*II-*Bam*HI, 498 bp]Ω[pMS4Δ4.5 *Afl*II-*Hin*dIII, 421 bp, *Hin*dIII-*Bam*HI adapter[a]]	7045–4672	This work
pMS4Δ3th	pMS4Δ3 Ω[pTZ1106His *Nde*I-*Nde*I, 368 bp]	6255–4596	This work
pMS4Δ3.1th	pMS4Δ3th Δ[*Afl*II-*Hin*dIII, 527 bp]Ω[*Afl*II-*Hin*dIII adapter[a]]	6255–5083	This work
pMS4Δ4.3th	pMS4Δ4.3 Ω[pTZ1106His *Nde*I-*Nde*I, 368 bp]	5097–4596	This work
pST4Δ1	pDB17HE Δ[*Nde*I-*Bam*HI, 2,861 bp]Ω[PCR pMS4Δ1 *Nde*I-*Asc*I, 472 bp; pMS4Δ1 *Asc*I-*Bam*HI, 1,907 bp]	7045–4596	This work
pTZ1106His	pMS119HE Ω[*Nde*I-*Nde*I, *trxA*-His$_6$, 368 bp]		30
pSTP4ori	pMS119EH Ω[P4 *Ssp*I-*Bst*NI, 361 bp]	9105–9465	This work
Phages			
M13 mMS4Δ1	M13mp18 Ω[pMS4Δ1 *Eco*RI-*Hin*dIII, 2,495 bp]	7045–4596	27
P4 *vir1*	Immunity insensitive		17
P4 *vir1* αE214Q	Primase-null		27
P4 *CI405*	Does not lysogenize		4
P4 *CI405* α *am105*	Replication deficient		D. Ghisotti

[a] See Table 2.

AGGAAACAGAATTCGAGC and TATATGAAGCTTAGTCGCCGTAGCT TTCCTCTTTC (P4 coordinates 4672 to 4693). To create pMS4Δ1.5th, the 498-bp *Afl*II-*Bam*HI fragment of pMS4Δ1th was exchanged for the 421-bp *Afl*II-*Hin*dIII fragment of pMS4Δ4.5 and a *Hin*dIII-*Bam*HI adapter. To create pMS4Δ3.1th, the 527-bp *Afl*II-*Hin*dIII fragment of pMS4Δ3th was exchanged for an *Afl*II-*Hin*dIII adapter (TTAAGGAC**TAG**A, AGCTT**CTA**GTCC) supplying a stop codon. The stop codon and the respective bases of the complementary strand are shown in boldface.

The C35 and C57 mutant *trxA*-His$_6$-α (α-th) fusions were constructed by replacing the 472-bp *Nde*I-*Asc*I fragment of pMS4Δ1th by the mutated counterparts generated by PCR with the mutated pMS4Δ1 plasmid as the template. The NBS mutant-th fusions were constructed by replacing the 560-bp *Dra*III-*Afl*II fragment of pMS4Δ1th with the mutated counterparts. Other α-th fusions were constructed by inserting the 368-bp *Nde*I-*Nde*I fragment of pTZ1106His encoding thioredoxin A-His$_6$ into the respective α-encoding plasmid via its *Nde*I recognition site, which is part of the start codon.

pSTP4ori was constructed by inserting the P4 origin (P4 nucleotides 9105 to

TABLE 2. Nucleotide sequences of adapters used

Adapter	Sequence
*Afl*II-*Hin*dIII	TTAAGGACTAGA CCTGATCTTCGA
*Dde*I-HindIII	TCAGACTGA CTGACTTCGA
*Hin*dIII-*Bam*HI	AGCTTGGAAGGG ACCTTCCCCTAG
*Nde*I-*Msc*I	TATGCTCCTTTCTCTGG ACGAGGAAAGAGACC
*Nde*I-*Sma*I	TATGCAGGAGTTTGCCC ACGTCCTGAAACGGG
*Nde*I-*Afl*II	TATGCCGCAGC ACGGCGTCGAATT

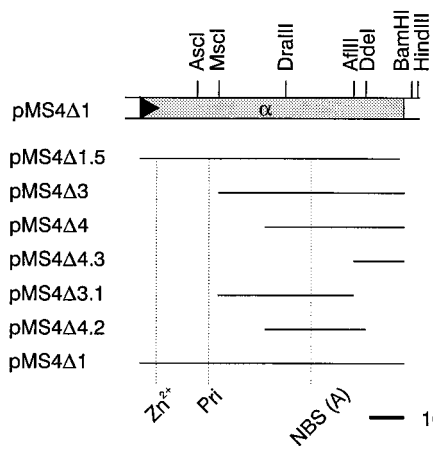

gpα amino acid position	ATPase	Helicase	*ori*/*crr* binding
1-766	(+)	±	+
239-777	+	+	+
370-777	−	−	+
625-777	nt	nt	+
239-630	−	−	−
370-663	−	nt	−
1-777	+	+	+

FIG. 1. Properties of truncated α proteins. The bar in the upper part shows a physical map of the α gene contained in pMS4Δ1. The locations of relevant restriction sites are marked. The 5′ end of α is indicated by a triangle. The lines represent the extents of the truncated α proteins encoded by the respective plasmids. The potential metal ion binding domain (Zn^{2+}), the EGYATA primase motif (Pri), and the type A NBS are marked. For the overproduced proteins, the table summarizes the in vitro activities. +, activity retained; −, no activity; nt, not tested.

9465) contained within the 412-bp *Eco*RI-*Hin*dIII fragment of M13 derivative mMSP4ori (30) into pMS119EH.

Purification of α-th proteins. A 500-ml culture of SCS1 harboring the respective α-th-overexpressing plasmid was grown at 37 or 30°C with shaking. At an A_{600} of 0.5, isopropyl-β-D-thiogalactopyranoside was added to 1 mM. Shaking was continued for 5 h. Cells were centrifuged at 4,000 × *g* for 10 min, resuspended in 1 mM spermidine Tris hydrochloride–200 mM NaCl–2 mM EDTA (pH 7.5) (1 g [wet weight] of cells in 5 ml), and frozen in liquid nitrogen. All subsequent steps were performed at 0 to 4°C. Frozen cells were thawed (3 g in 15 ml) and adjusted to 40 mM Tris-HCl (pH 7.6)–4% sucrose–0.13% Brij 58–1 M NaCl–2.5 mM dithiothreitol (DTT)–0.3 mg of lysozyme per ml. Following incubation for 1 h, the highly viscous lysate was centrifuged at 100,000 × *g* for 60 min.

When gpα-th derivatives were poorly soluble, the following procedure was used. The pellet was washed twice with 1 M NaCl in buffer A (20 mM Tris-HCl [pH 7.6], 2.5 mM DTT, 1 mM EDTA) by rigid homogenization to remove soluble proteins. Then the pellet was resuspended twice in 6 M urea–1 M NaCl in buffer A to dissolve gpα-th proteins. The supernatants of the two urea steps were combined, and the proteins were precipitated with ammonium sulfate at 60% saturation. The pellet was solubilized in buffer B (6 M urea, 50 mM sodium phosphate [pH 8.0], 300 mM NaCl) containing 20 mM imidazole-HCl (pH 8.0) and dialyzed against buffer B–20 mM imidazole-HCl (pH 8.0). This fraction was applied at 5 ml/h to a Ni^{2+}-nitrilotriacetic acid column (0.9 by 7.5 cm) equilibrated with buffer B–20 mM imidazole-HCl (pH 8.0). The column was washed with 20 ml of buffer B–20 mM imidazole-HCl (pH 8.0). Proteins were eluted with 250 mM imidazole-HCl (pH 8.0) in buffer B. Peak fractions containing α-th were pooled, dialyzed four times against buffer C (20 mM Tris-HCl [pH 7.6], 50 mM NaCl, 1 mM DTT, 1 mM EDTA) to renature the protein, and then dialyzed two times against a 10-fold volume of buffer C to remove residual urea. The fraction was concentrated by dialysis against 20% (wt/vol) polyethylene glycol 20,000, dialyzed against 50% (wt/vol) glycerol in buffer C, and stored at −20°C.

When α-th derivatives were soluble, the following procedure was used. After centrifugation of the cell lysate, proteins were dissolved in buffer A containing 1 M NaCl. Proteins were then precipitated with ammonium sulfate as described above. The pellet was solubilized in buffer D (50 mM sodium phosphate [pH 8.0], 500 mM NaCl) containing 20 mM imidazole-HCl (pH 8.0) and dialyzed against buffer D–20 mM imidazole-HCl (pH 8.0). The dialysate was applied at 5 ml/h to a Ni^{2+}-nitrilotriacetic acid column (0.9 by 7.5 cm) equilibrated with buffer D–20 mM imidazole-HCl (pH 8.0). The column was washed with 20 ml of buffer D–20 mM imidazole-HCl (pH 8.0). Proteins were eluted with 250 mM imidazole-HCl (pH 8.0) in buffer D. Peak fractions containing α-th derivatives were pooled, concentrated by dialysis against 20% (wt/vol) polyethylene glycol 20,000, dialyzed against 50% (wt/vol) glycerol in buffer C–500 mM NaCl, and stored at −20°C.

ATPase assay. The standard reaction mixtures (20 μl) contained 20 mM Tris-HCl (pH 7.6), 100 mM NaCl, 2 mM $MgCl_2$, 1 mM DTT, 100 nCi of [γ-^{32}P]ATP (3,000 Ci/mmol), 200 μM ATP, and 50 μg of bovine serum albumin per ml. When appropriate, 1 μg of viral M13mp18 DNA was added. After incubation at 30°C for 15 min, the reactions were terminated by adding EDTA to 10 mM. A 2-μl aliquot of the mixture was analyzed by thin-layer chromatography using Polygram CEL 300 PEI plates, which were developed in 1 M LiCl–1 M acetic acid.

Helicase assay. The forked helicase substrate used was described by Crute et al. (6). To viral M13mp18 DNA, a 5′ ^{32}P-labeled oligodeoxynucleotide was annealed, resulting in a double-stranded portion of 23 bp and 22 unpaired nucleotides at the 5′ end. The standard reaction mixtures (20 μl) contained 20 mM Tris-HCl (pH 7.6), 100 mM NaCl, 5 mM $MgCl_2$, 1 mM DTT, 4 mM ATP, 50 μg of bovine serum albumin per ml, 0.05% Brij 58, and 40 fmol of helicase substrate. After incubation at 30°C for 20 min, the reactions were terminated by adjusting the mixture to 25 mM EDTA, 0.25% SDS, and proteinase K at 0.1 mg/ml. Following incubation for additional 5 min at 30°C, the samples were electrophoresed on 10% polyacrylamide gels in 89 mM Tris-borate (pH 8.3)–1 mM EDTA at 8 V/cm. Products were visualized by storage phosphor autoradiography (11) and analyzed with ImageQuant software, version 3.3 (Molecular Dynamics).

Primase assay. DNA primase activity was assayed in vitro in the presence of rifampin and [^{3}H]dTTP by using an extract of *E. coli dnaB dnaC* mutant strain BC1304 as described previously (13, 14). Viral fd DNA was used as the template for the priming of complementary-strand synthesis. dTMP incorporated in 30 min at 30°C into acid-insoluble material was measured.

Fragment retardation assay. The source for P4 *ori* fragments was pSTP4ori, which contains the 361-bp *ori* fragment inserted into the multiple cloning site (Table 1). Digestion with *Eco*RI, *Hin*dIII, and *Mlu*I yielded an *ori*-containing fragment of 412 bp and additional fragments of 631 and 3,446 bp. After 5′ labeling with [γ-^{32}P]ATP and T4 polynucleotide kinase, the fragments (1 nM each) were incubated with increasing amounts of α protein derivative in a total volume of 20 μl of buffer containing 20 mM Tris-HCl (pH 7.6), 100 mM NaCl, 750 μg of bovine serum albumin per ml, and 75 μg of calf thymus DNA per ml and electrophoresed on nondenaturing 3.5% polyacrylamide gels as described previously (33). Following electrophoresis, the ^{32}P-labeled DNA bands were visualized by the storage phosphor method (11) and analyzed with ImageQuant software, version 4.1b (Molecular Dynamics).

Complementation tests. Complementation studies with plasmids were done as described previously (32).

RESULTS

Construction of truncated α genes. The primase domain occupies the N-terminal third of gpα containing the primase motif -EGYATA-, which is essential for primase activity (27, 32). Specific DNA binding was assigned to the C-terminal 265 amino acids by deletion analysis (32). To define the ATPase, helicase, and specific DNA binding domain in more detail, we constructed a series of deletions at the 5′ and 3′ ends of the α gene (see Materials and Methods and Fig. 1).

Overproduction of α-th fusions. Several mutant α proteins that are truncated or that carry single amino acid exchanges are poorly soluble in nondenaturing buffers. Since TrxA fusions were described to circumvent the formation of inclusion bodies of certain proteins in the *E. coli* cytoplasm (15), we fused the N terminus of each α protein to TrxA to give α-th derivatives (see Materials and Methods). Transcription was controlled by the P*tac*/*lacI* system. Each α-th gene was preceded by the phage T7 *gene10* Shine-Dalgarno sequence for

TABLE 3. Complementation of primase-null P4 phage by plasmids encoding α derivatives[a]

P4 *vir1* phage	Burst size (phage/cell) with plasmid:			
	pMS119EH (vector)	pMS4Δ1 (wild-type α)	pMS4Δ1th (TrxA-His_6-α)	pMS4Δ1C35H
Wild-type α	26 ± 7	46 ± 14	22 ± 6	24 ± 10
αE214Q	0.5 ± 0.1	40 ± 17	23 ± 5	0.7 ± 0.4

[a] *E. coli* C-2309 [*dnaG3* (P2 *lg*)] was infected at 42°C. Values are averages of at least two experiments.

efficient translation initiation. For facilitated purification via a Ni^{2+}-chelating matrix, we used a thioredoxin derivative containing a His_6 tag. Although some of the α-th proteins formed inclusion bodies at 30°C, they could be solubilized in buffer containing 6 M urea and renatured in physiological buffers (see Materials and Methods). To test for renaturation, gpα-th was purified under nondenaturing and under denaturing conditions and assayed for ATPase, helicase, and specific DNA binding activities. Since those functions were restored (see below), we concluded that the renaturation procedure applied would be suitable for the poorly soluble gpα-th derivatives.

The N-terminal thioredoxin A moiety reduces primase activity. The primase domain occupies the N-terminal third of gpα (32). Therefore, we wondered whether the Trx-His_6 modification influences the primase activity. To determine whether α-th molecules have primase activity in vivo, we used pMS4Δ1th, which encodes α-th, to complement P4 phage carrying an E214Q mutation in the primase motif. This phage cannot grow in an *E. coli dnaG ts* strain at 42°C. The α-th protein appears to inhibit the growth of wild-type P4 by a factor of 2. Under these conditions, the primase-defective phage is complemented half as well by α-th as by wild-type α (Table 3). This result suggests that in vivo primase activity is reduced, but not eliminated, in gpα-th.

In contrast to this result, the primase activity of purified gpα-th measured in vitro (see Materials and Methods) was diminished to values slightly above background (Fig. 2). We speculated that the loss of activity was due to steric hindrance or misfolding promoted by the N-terminal modification. Therefore, the Trx-His_6 moiety was cleaved off with enteropeptidase. The cleavage reaction resulted in two large major products; the larger one had an apparent mass comparable to that of gpα. This molecule started at gpα amino acid position 2, whereas the smaller major species started at position 66, as demonstrated by microsequencing. Furthermore, several minor products were detected. The mixture of α molecules retained primase activity (Fig. 2). This finding is evidence that the free gpα N terminus is required for primase activity.

The N-terminal Trx-His_6 moiety of α fusion proteins does not inhibit ATPase, helicase, and specific DNA binding activities. gpα functions might be inhibited by the modified N terminus, due to disturbed tertiary structure of the protein or due to steric hindrance. To determine whether gpα with the N-terminal modification is suitable for tests of the purified proteins for ATPase, helicase, and specific DNA binding activities, we compared these functions of gpα and gpα-th. gpα-th was active in hydrolyzing ATP in the presence and absence of single-stranded DNA. Without DNA, gpα-th was approximately 50% more active than gpα at a concentration of 50 nM (Fig. 3). However, gpα-th was less stimulated by single-stranded DNA than gpα. To examine whether the stimulation of the ATPase activity in the presence of single-stranded DNA (ssDNA) could be recovered, the Trx-His_6 moiety of gpα-th was cleaved off with enteropeptidase. As a control, gpα-th was also incubated in enteropeptidase buffer without peptidase. We could not detect any significant differences in the ATPase activity of the processed α protein, the control incubated without protease, and untreated gpα-th. In contrast to wild-type gpα, the ATPase activity of the enteropeptidase-digested gpα-th was not stimulated by the addition of ssDNA (data not shown).

The helicase activities of gpα and gpα-th were similar (Fig. 4). For both proteins, the maximum amount of oligonucleotide displaced was found at a protein concentration of approximately 250 nM. Furthermore, gpα-th still binds specifically to *ori* (Fig. 5) and *crr* (not shown). The results show that the Trx-His_6 moiety does not greatly inhibit the ATPase, helicase, and specific DNA binding activities of the α protein, suggesting a structure of gpα-th similar to that of gpα.

Amino acid residues G506 and K507 of NBS type A are essential for the gpα-catalyzed hydrolysis of ATP. α proteins with amino acid exchanges within the core amino acid sequence GKS of the NBS motif that alter the chemical character of the side chain could not support propagation of an α-null P4 phage (32). The exchanges were G506E, K507A, K507D, K507Q, and K507T. To test whether the replication deficiency is due to reduced ATPase and/or helicase activity, each mutant gpα fused to TrxA-His_6 was purified and analyzed for its ability to hydrolyze ATP. Except for gpαK507T-th, no ATP hydrolysis

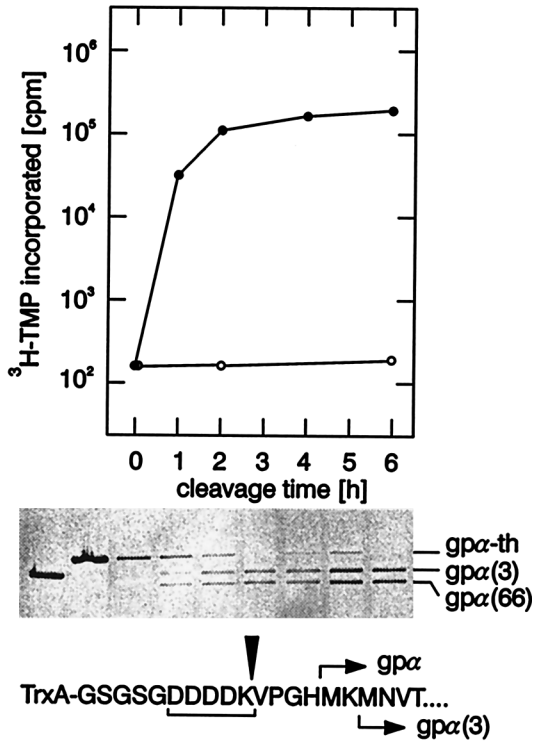

FIG. 2. Primase activity of gpα-th. Thirty micrograms of gpα-th in 40 μl of buffer consisting of 50 mM Tris-HCl (pH 8.0), 50 mM $CaCl_2$, and 100 mM NaCl was cleaved by enteropeptidase at 37°C. A time course of the reaction is shown. The products were analyzed on denaturing polyacrylamide gels containing 0.1% SDS. An electronic image of the Coomassie blue-stained gel is shown below the graph. The aliquots were analyzed for primase activity as described in Materials and Methods. [^{3}H]TMP incorporated into acid-precipitable material was plotted against the cleavage time. Closed circles, enteropeptidase present; open circles, enteropeptidase omitted. At the bottom, the linkage of TrxA and gpα is shown. The bracket and the wedge denote the recognition site and the cleavage site of the enteropeptidase. The recognition site is preceded by a linker.

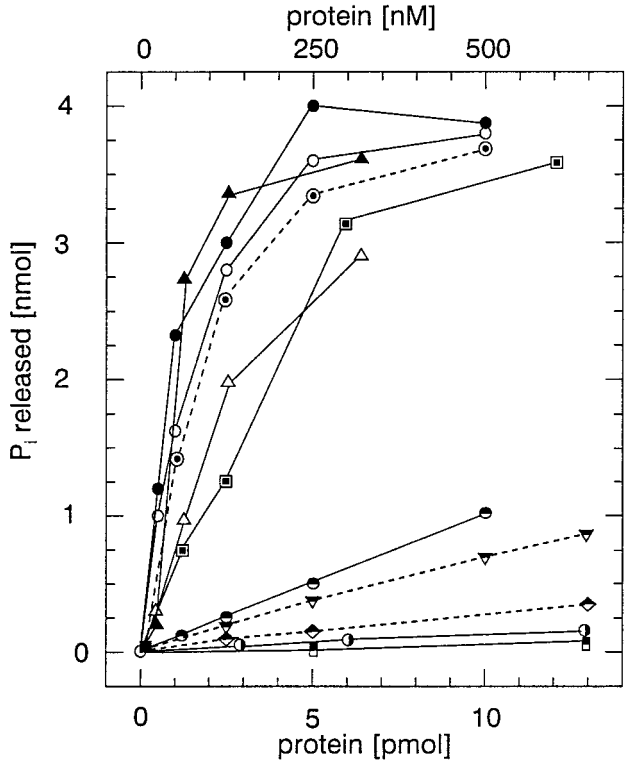

FIG. 3. ATPase activities of α proteins. Mutant α proteins were assayed for ATPase activity in the presence or absence of ssDNA as described in Materials and Methods. Symbols composed of black and white indicate that the presence or absence of DNA did not influence the ATPase activity. The broken lines are assigned to α proteins with single amino acid exchanges. For each protein, the values plotted are averaged from three experiments. Experiments with proteins defective in triphosphate hydrolysis were repeated twice. Symbols: △, gpα without ssDNA; ▲, gpα with ssDNA; ○, gpα-th without ssDNA; ●, gpα-th with ssDNA; ◓, gpαΔ1.5-th; ⊡, gpαΔ3-th; ◑, gpαΔ4-th; ⬒, gpαΔ3.1-th; ▽, gpαC57G-th; ◈, gpαC35G-th or gpαK507T-th; ⊙, gpαC35H-th. ATP hydrolysis of gpαG506E, gpαG506E-th, gpαK507A-th, and gpαK507D-th was indistinguishable from background and therefore was omitted from the graph.

could be detected for the mutant α-th proteins and for gpαG506E. For gpαK507T-th, the ATPase activity detected was reduced by approximately 2 orders of magnitude compared to gpα-th or wild-type gpα at a protein concentration of 125 nM in the presence of single-stranded DNA (Fig. 3).

The G506 and K507 mutant α proteins are defective in unwinding a forked helicase substrate. gpα unwinds unforked helicase substrates less efficiently than forked substrates that have some of the structural features of a replication fork (33). Although the G506 and K507 mutant proteins (see above) do not hydrolyze ATP, it could not be ruled out that a replication fork-like structure complexed with gpα restores the ATPase activity that drives unwinding. Using the substrate described in Materials and Methods, no displacement of the oligonucleotide could be detected, demonstrating the importance of the exchanged residues for ATPase or helicase function. Also, the residual ATP hydrolyzing activity of gpαK507T-th was not sufficient to fuel unwinding (data not shown).

ATPase and helicase activities of gpα require the specific DNA binding domain. The C-terminal half of gpα contains three short stretches of amino acid residues, including the nucleotide binding fold (type A), that are conserved in the putative NTPase domain of potential helicases of small DNA and RNA viruses (8). Since these segments are centered between amino acid residues 496 and 592 (Fig. 1), it was speculated that the C-terminal half of gpα might function at least as an ATPase. To locate the ATPase and helicase domain, we made a series of N-terminal and C-terminal truncations (Fig. 1). The histidine-tagged Trx-gpα fusion proteins were purified and assayed for ATPase, helicase, and specific DNA binding activities (see below). The ATPase activity of gpαΔ3-th (gpα positions 239 to 777) at a protein concentration of 50 nM was reduced by a factor of 4 compared to gpα-th (Fig. 3). This reduced hydrolyzing activity was reflected by the reduced helicase activity. Even at higher protein concentrations, the percentage of oligonucleotide displaced did not reach that of gpα-th (Fig. 4). The ATPase activity of gpαΔ4-th (gpα positions 370 to 777) was slightly above background. The latter was unable to displace oligonucleotides. These results demonstrate that the presence of the three segments conserved in potential helicases of small viruses is not sufficient for triphosphate hydrolysis. Furthermore, the gpα N-terminal half that gpαΔ4-th lacks is required for wild-type ATPase and helicase functions.

The C-terminal truncated version of gpαΔ3-th, gpαΔ3.1-th (gpα positions 239 to 630) lacking the specific DNA binding domain (see below), possessed neither ATPase nor helicase activity. This finding indicates that the helicase domain overlaps or includes the specific DNA binding domain. Therefore, we made a gpα construct lacking the very 11 C-terminal amino acid residues. This protein, gpαΔ1.5-th (gpα positions 1 to 766), was one-quarter as active in hydrolyzing ATP as gpαΔ3-th (Fig. 3). The unwinding activity was slightly above background and could not be enhanced by increasing the protein concentration, demonstrating that the C-terminal end is essential for α helicase.

Helicase-defective mutations of amino acids 506 and 507 abolish the ability to support growth of P4 α amber mutants (32). Thus, we expected that deletion of the C-terminal 11 amino acid residues would prevent complementation of an α amber phage. The results summarized in Table 4 show that this

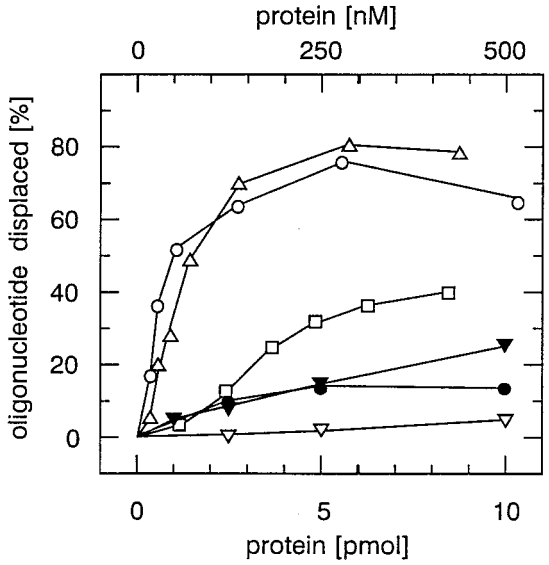

FIG. 4. Helicase activities of α proteins. Several α mutant proteins were assayed for the ability to displace an oligonucleotide bound to viral M13mp18 DNA as described in Materials and Methods. The percentage of the oligonucleotide displaced was determined by volume integration of the signals produced by the substrate and the product, using ImageQuant software (Molecular Dynamics). For each protein, the values plotted are averaged from three experiments. △, wild-type gpα; ○, gpα-th; ●, gpαΔ1.5-th; □, gpαΔ3-th; ▽, gpαC57G-th; ▼, gpαC35H-th.

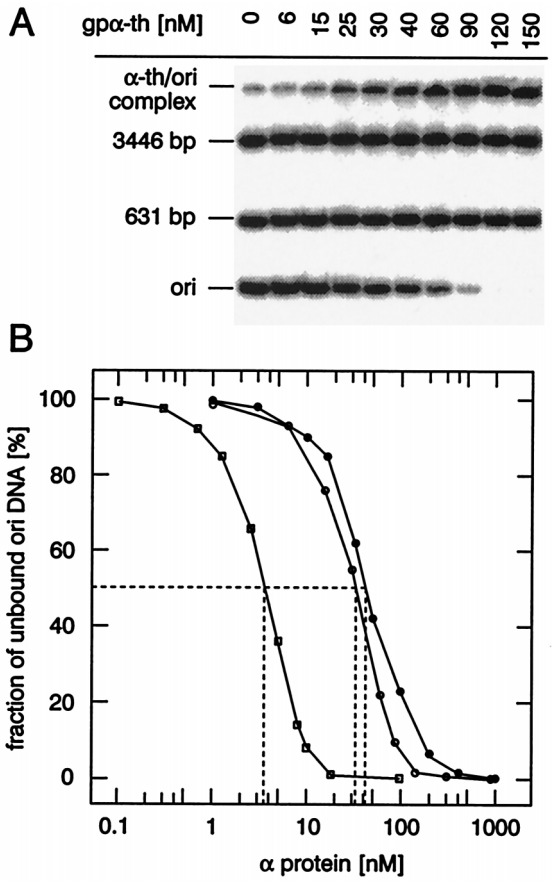

FIG. 5. Equilibrium binding of gpα derivatives to P4 *ori*. (A) ^{32}P-labeled P4 *ori* DNA fragment (P4 nucleotides 9105 to 9465) and competitor DNA fragments were incubated with increasing amounts of gpα-th and electrophoresed as outlined in Materials and Methods. A printout of the electronic image of one representative autoradiograph is shown. (B) Determination of the equilibrium dissociation constants of α proteins. ○, gpα-th; ●, gpαΔ1.5-th; □, gpαΔ4.3-th. For each protein, the values plotted are averaged from at least three experiments.

is the case and that deletions of four or seven amino acids did not affect complementation.

Do amino acid replacements of C35 or C57 influence the functional structure of the ATPase/helicase domain? For full ATPase and helicase function, gpα requires the N-terminal domain (see above) that includes the cysteine-rich potential metal ion binding motif. To determine whether this domain plays a role in ATPase and/or helicase function, the following amino acid exchanges were made: C35G, C35H, and C57G. The ATPase activity of gpαC35G-th and gpαC57G-th at a concentration of 50 nM was reduced by 1 to 2 orders of magnitude compared to gpα-th (Fig. 3). At a given concentration, the C35G protein was less active than C57G. In agreement to these results, the C35G polypeptide was completely inactive in displacing the oligonucleotide from the helicase substrate, and the C57G protein was almost inactive (Fig. 4). The triphosphate hydrolyzing activity of gpαC35H-th was slightly less than but comparable to that of gpα-th. However, the ability of this derivative to displace the oligonucleotide from the helicase substrate at 50 mM protein concentration was reduced 10-fold compared to that of gpα-th. This result indicates that in the C35H molecule, ATPase and helicase activities are uncoupled. Since gpαΔ3-th lacking the cysteine-rich motif hydrolyzes ATP, albeit less efficiently than does gpα-th, this motif could not be essential for ATPase function. It must be considered that the C→G exchanges at the N terminus caused structural distortions affecting native protein folding required for ATPase or helicase function. The mutations did not affect specific DNA binding, indicating that the specific DNA binding domain at the C-terminal end is in its native conformation. By adding zinc ions, we tried to stabilize the protein to restore the enzymatic functions. However, at $ZnCl_2$ concentrations of 10 nM to 100 μM, no increase in ATPase or helicase activity was observed. Both functions of gpα-th were inhibited at 100 μM (data not shown).

To gain insight into the in vivo situation, we analyzed whether a replication-deficient P4 α amber phage could be complemented with gpαC35H delivered from a plasmid. We used P4 α *am105*, which has a TAG mutation near the 5′ end of the α gene (32). When the plasmid-borne α gene carries the primase-null E214Q allele, P4 progeny is produced at 70% of the level with wild-type gpα. This may be due to the activity of the *E. coli* DnaG primase (27). In contrast, the helicase-null gpαK507T does not complement the replication-deficient α mutant phage. The αC35H protein was fourfold less efficient than wild type in supporting phage growth (Table 4). Thus, the C35H mutation appears to reduce the helicase activity of gpα in vivo.

Cysteine 35 of the cysteine-rich motif is essential for primase activity. Several prokaryotic DNA primases, for instance, T7 gp4, T4 gp61, or DnaG proteins of several bacterial species, contain a cysteine-rich motif similar to that of gpα (18, 31). For T7 gp4, it was shown that this motif binds zinc ions and is essential for primase function (18) but not for helicase activity. P4 gpαC35G and gpαC57G were shown to be primase deficient in vivo and in vitro (32). Since this deficiency might be due to a structural distortion, an additional mutant protein, gpαC35H, was analyzed. The cysteine-to-histidine exchange should retain the potential coordination of zinc ions and therefore retain the native conformation of the protein. However, in cell extracts containing gpαC35H, primase activity was not detectable. To confirm this result in vivo, we tested whether gpαC35H supports growth of the primase-null P4 phage αE214Q. Since growth of this phage is prevented only when the host primase DnaG is destroyed, we used a strain carrying the *dnaG3 ts* allele at the nonpermissive temperature of 42°C. In the presence of pMS4Δ1C35H, the growth of P4 wild-type phage was not inhibited (Table 3), indicating that no abortive

TABLE 4. Complementation of gpα-defective P4 phage by various P4 α plasmids[a]

P4 *CI405* phage	Burst size (phage/cell) with pMS4 plasmids							
	pMS119EH (vector)	Δ1 (wild-type α)	Δ1.40 (4[b])	Δ1.41 (7)	Δ1.5 (11)	Δ1C35H	Δ1E214Q	Δ1K507T
Wild-type α	275 ± 71	198 ± 18	201 ± 14	233 ± 14	231 ± 6	268 ± 32	350 ± 30	238 ± 25
α *am105*	0.2 ± 0.0	211 ± 14	229 ± 47	194 ± 27	7.4 ± 3.7	58 ± 5	243 ± 17	0.1 ± 0.05

[a] *E. coli* C-2422 was infected at 37°C. Values are averages of at least two experiments.
[b] The number of C-terminal amino acid residues lacking.

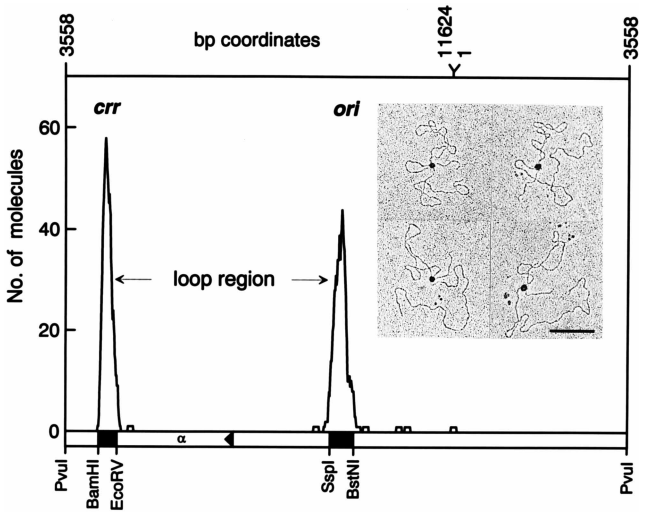

FIG. 6. Electron microscopy of complexes of gpαΔ4.3-th and P4 DNA. The complexes were formed by incubating supercoiled P4 DNA with gpαΔ4.3-th as described previously (33). Following fixation with glutaraldehyde and gel filtration (Sepharose 4 BCl), the DNA was cut with *Pvu*I and prepared for electron microscopy as outlined by Pérez-Martin et al. (21). The histogram depicts the frequency distribution of protein bound to *ori* and *crr* within a range of ±0.5% of the DNA length. One hundred eleven complexes showing a looped region were analyzed and aligned. In the lower bar, which represents the P4 genome of 11,624 bp, the positions of the α gene, *ori*, and *crr* are indicated. Relevant restriction sites are marked. Inset, representative electron micrographs of looped gpαΔ4.3-th–P4 DNA complexes. The bar represents 1 kb.

complex formation with gpαC35H occurs. The primase-null mutation of P4 αE214Q could not be complemented by gpαC35H. This finding suggests either that primer synthesis of gpαC35H is affected or that the protein cannot interact with the host elongation system, e.g., DNA polymerase III holoenzyme.

Amino acids 625 to 766 are sufficient for specific DNA binding. The *ori* and *crr* binding ability of gpα was assigned to its C terminus (32). To localize the specific DNA binding domain more precisely, two gpα-th derivatives were analyzed for specific complex formation by fragment retardation on gels. gpαΔ4.3-th contains gpα amino acid residues 625 to 777, whereas gpαΔ1.5-th contains residues 1 to 766. Each construct was still able to specifically bind *ori*-DNA (Fig. 5) or *crr*-DNA (not shown). Thus, the specific DNA binding domain lies between residues 625 and 766. The complexes of *ori* and α protein derivatives or wild-type protein were detected at the bottom of the gel wells (Fig. 5A and reference 33). This result indicates that large DNA-protein aggregates that could not enter either low-percentage polyacrylamide gels or agarose gels were formed (data not shown). This observation, also made for gpαΔ4.3-th and gpαΔ1.5-th, led to the conclusion that amino acid residues 625 to 766 not only specify DNA binding but also contain the domain responsible for the oligomerization of gpα by protein-protein interactions (see below).

To analyze whether the amino acid sequences flanking residues 625 to 766 add on the strength of binding, the apparent equilibrium dissociation constants $K_{d(app)}$ for gpαΔ1-th, gpαΔ1.5-th, and gpαΔ4.3-th were determined by the method of Carey (5). For this analysis, a fixed concentration of defined DNA fragments (see Materials and Methods) and increasing concentrations of α proteins spanning 4 orders of magnitude were used. Since the concentration of the fragment was much lower than that of the protein required for half-maximal binding, the K_d is approximately equal to the protein concentration at which half of the *ori* fragment was bound specifically. The Bjerrum plot of the fraction of free *ori* fragment versus log of α protein concentration is shown in Fig. 5. The K_d values determined for gpα-th and gpαΔ1.5-th are similar (32 and 41 nM), whereas that for gpαΔ4.3-th is 1 order of magnitude lower (3.5 nM). This result demonstrates that amino acid residues outside the 625–766 domain are not responsible for the specificity of DNA binding, because the lower K_d value of gpαΔ4.3-th indicates an increase of affinity.

In the electron microscope, loop formation between *ori* and *crr* was detected in the presence of gpα and supercoiled or linear P4 DNA (31). Therefore, we wondered whether gpαΔ4.3-th could mediate the formation of such structures. The analysis of P4 DNA–gpαΔ4.3-th complexes demonstrated protein-mediated looping between *ori* and *crr* (Fig. 6). Similar results were obtained with gpαΔ1.5-th (data not shown). This result again indicates that gpα amino acid residues 625 to 766 contain the domain for the specific protein-DNA interaction. Furthermore, these residues specify the domain required for the oligomerization of α molecules, since the large complex structures of gpαΔ4.3-th bridging *ori* and *crr* were also observed with α wild-type protein (31). In addition, this domain is also involved in interacting with the P4 Cnr protein (30), which regulates the P4 copy number (28).

DISCUSSION

The primase, helicase, and DNA binding activities of the P4 phage α protein have been mapped to the amino terminus, middle, and C terminus of gpα, respectively (27, 32). In this report, we have located these activities with greater precision (Fig. 7). The DNA binding activity is the first to be used in vivo. It is contained in a fragment of 141 amino acids, near the carboxyl terminus. To solubilize this fragment, we fused it to thioredoxin containing a histidine tag (Trx-His_6), with Trx-His_6 at the amino terminus. This fusion protein binds specifically to the origin of replication and to *crr*, causing formation of a looped structure in vitro. The existence of such a loop implies an oligomeric structure for gpα in the DNA-protein complex, and it predicts that the oligomerization domain is also con-

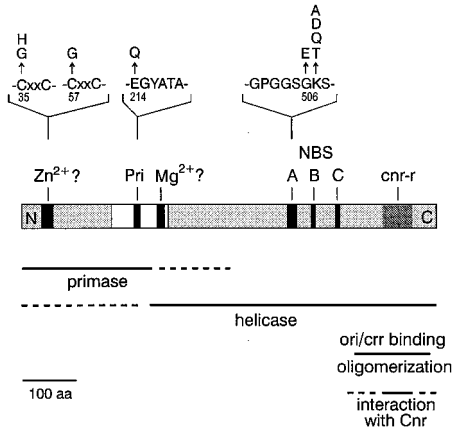

FIG. 7. Domain structure of gpα. The bar represents the α protein. Highlighted in white is the segment that has similarity to primases of IncI and IncP plasmids. The locations of the potential Zn^{2+} binding motif, the primase motif -EGYATA-, the potential Mg^{2+} binding motif conserved in polymerases, and the sequence motifs conserved in the putative NTPase domain (NBS) of potential helicases of small DNA and RNA viruses are indicated. Oligomerization refers to the ability to form large protein-DNA complexes. The cnr-r (Cnr-resistant) domain defined by mutagenesis probably interacts with the P4 Cnr protein. aa, amino acids.

tained in this polypeptide (Fig. 7). It is not clear whether oligomerization of gpα requires DNA binding or whether oligomerization occurs in the absence of DNA.

Electron microscopic studies using the following gpα derivatives and P4 DNA all confirmed specific binding to *ori* and *crr*, mediating loop formation: wild-type protein (31), gpαΔ1.5-th, gpαΔ4-th, gpαΔ4.1-th (data not shown), and gpαΔ4.3-th (Fig. 6). In assays using wild-type gpα, the double peak detected at *crr* (31) reflects binding to either of the two 120-bp repeats, that contains the multiple octameric binding targets. Such a doublet was not observed with gpαΔ4.3-th (Fig. 6). Since the protein aggregates of the gpαΔ4.3-th–P4 DNA complexes were slightly larger than those obtained with wild-type α protein, the single peak probably was a result of reduced resolution in measurement.

The K_d value of gpαΔ4.3-th, which is 1 order of magnitude below those determined for gpαΔ1.5-th and gpα-th, shows that the isolated domain required for specific DNA binding has a higher affinity to its target than the complete α protein. Therefore, it could be assumed that the inherent potential for *ori* binding is not expressed in the complete gpα but may be improved by interaction with another P4-encoded protein. P4 Cnr stimulates binding of gpα to *ori*, hence providing a regulatory mechanism for initiation of P4 replication (30).

Once gpα has bound to *ori* and *crr*, its helicase activity must unwind the AT-rich region of *ori*. Mutations at amino acids 506 and 507, in the type A NTP-binding motif, abolish both the NTPase and helicase activities. However, the helicase activity is not confined to this region alone. Its activity is greatly reduced by deletion of 11 amino acids from the carboxyl terminus, it is abolished by a C35G or a C57G mutation in the potential zinc binding motif near the N terminus, and it is reduced at least fourfold by a C35H mutation in the potential zinc binding motif near the N terminus.

Since 11 C-terminal amino acid residues are required for efficient helicase but not for specific DNA binding activity, the helicase domain overlaps that for specific DNA binding. A similar arrangement was also described for the simian virus 40 large T antigen, which combines origin recognition and 3′→5′ helicase function as does gpα. This multifunctional eukaryotic protein controlling progeny requires approximately three-quarters of the polypeptide for helicase activity, which includes the specific DNA binding domain (7).

The helicase and ATPase activities of gpαC35H-th are uncoupled, since the reduction in unwinding did not correspond to the reduced ATP hydrolysis. Thus, the overall conformation of gpα must be rigorously maintained in order to maximize helicase activity. Uncoupling of ATPase and helicase function was also reported for the *E. coli* PriA protein (29). Within the cysteine-rich motif of PriA (-CxxC-x_5-CxxC-x_{14}-CxxC-x_9-CxxC-), differing from that of gpα (-CxxC-x_{18}-CxxC-), various single cysteine residues were changed to glycine. In the presence of ssDNA containing a primosome assembly site, all three mutant proteins retain ATPase activity comparable to that of the wild-type protein at low protein concentrations. Of the three mutant proteins, however, only PriA C477G retained a 10-fold-reduced ability to displace an oligonucleotide from the helicase substrate. This activity could be stimulated by the addition of zinc ions. For gpα-th, we could not detect such an effect. This result indicates that the cysteine-rich motifs of gpα and PriA differ not only in amino acid sequence but probably also in three-dimensional structure.

Cysteine-rich, potential zinc binding motifs of the Cys_4 type are present in prokaryotic and eukaryotic primases. However, only phage T7 gp4 and *E. coli* DnaG protein have been shown to be zinc metalloproteins (18, 26). gp4 exists as a 63-kDa protein that combines primase and helicase activities and as a 56-kDa protein with helicase activity, which lacks the 63 N-terminal amino acid residues of the larger polypeptide. This N-terminal peptide contains the Zn^{2+} binding, cysteine-rich motif -CxxC-x_{17}-CxxC- (18). gp4 derivatives containing a C-to-S change within this motif were primase deficient; the helicase was approximately 10% as active as the wild-type protein. The addition of Zn^{2+} ions did not restore the enzymatic activities (18). These results are similar to ours obtained with gpαC35H. This finding demonstrates the importance of the cysteine-rich motif for primase and in addition for helicase activity.

Since zinc finger motifs in eukaryotic proteins recognizing specific nucleotide sequences are present in several copies, the single cysteine-rich motif of gpα might resemble an alternative metal binding motif, termed zinc ribbon (-CxxC-x_{24}-CxxC-), that was found in the N terminus of the human transcription elongation factor TFIIS (22).

The C35H mutation completely eliminates primase activity, whereas it only reduces helicase activity. This is not surprising, since primase activity has been associated with the amino-terminal half of gpα, which lacks helicase activity.

Because there are many ATPases in *E. coli*, we sought more highly purified gpα for analysis of its NTPase activity. We fused Trx-His_6 to the amino terminus of gpα, in order to utilize nickel affinity chromatography in purification. Purified gpα-th has no primase activity, as measured on single-stranded circular DNA in vitro. In contrast, gpα-th appears to have substantial in vivo primase activity in *E. coli dnaG3* cells, where P4 primase activity is essential for phage production at 42°C. We considered the possibility that the Trx-His_6 moiety was being removed from a fraction of the gpα-th molecules by proteolysis, generating active, cleaved gpα that was lost during our purification. However, we found no primase activity in the crude extract, making this possibility unlikely. Primase is the last of gpα's three activities to function on P4 DNA, following DNA binding and unwinding. It may be that the processes of DNA binding and DNA unwinding cause a change in conformation of gpα-th and that this conformational change relieves primase inhibition by Trx-His_6.

ACKNOWLEDGMENTS

The expert technical assistance of Marianne Schlicht is greatly appreciated. We thank Simona Türk for the construction of several plasmids, Daniela Ghisotti for kindly providing P4 *CI405 am105*, and Werner Schröder for N-terminal microsequencing of α proteins.

Work in our laboratories was supported by grant La 672/3-2 and by Sonderforschungsbereich grant 344/B2 of the Deutsche Forschungsgemeinschaft to E.L. and by grant AI-08722 from the National Institute of Allergy and Infectious Diseases to R.C.

REFERENCES

1. **Balzer, D., G. Ziegelin, W. Pansegrau, V. Kruft, and E. Lanka.** 1992. KorB protein of promiscuous plasmid RP4 recognizes inverted sequence repetitions in regions essential for conjugative plasmid transfer. Nucleic Acids Res. **20:**1851–1858.
2. **Bowden, D. W., R. S. Twersky, and R. Calendar.** 1975. *Escherichia coli* deoxyribonucleic acid synthesis mutants: their effect upon bacteriophage P2 and satellite bacteriophage P4 deoxyribonucleic acid synthesis. J. Bacteriol. **124:**167–175.
3. **Bullock, W. O., J. M. Fernandez, and J. M. Short.** 1987. XL1-Blue: a high efficiency plasmid transforming *recA Escherichia coli* strain with beta-galactosidase selection. BioTechniques **5:**376–378.
4. **Calendar, R., E. Ljungquist, G. Dehò, D. Usher, R. Goldstein, P. Youderian, G. Sironi, and E. Six.** 1981. Lysogenization by satellite phage P4. Virology **113:**20–28.
5. **Carey, J.** 1991. Gel retardation. Methods Enzymol. **208:**103–117.
6. **Crute, J. J., E. S. Mocarski, and I. R. Lehman.** 1988. A DNA helicase induced by herpes simplex virus type 1. Nucleic Acids Res. **16:**6585–6596.
7. **Fanning, E., and R. Knippers.** 1992. Structure and function of simian virus

40 large tumor antigen. Annu. Rev. Biochem. **61:**55–85.
8. **Gorbalenya, A. E., E. V. Koonin, and Y. I. Wolf.** 1990. A new superfamily of putative NTP-binding domains encoded by genomes of small DNA and RNA viruses. FEBS Lett. **262:**145–148.
9. **Halling, C. R., R. Calendar, G. E. Christie, E. C. Dale, G. Dehò, S. Finkel, J. Flensburg, D. Ghisotti, K. L. Kahn, K. B. Lane, C.-S. Lin, B. H. Lindqvist, L. S. Pierson III, E. W. Six, M. G. Sunshine, and R. Ziermann.** 1990. DNA sequence of satellite bacteriophage P4. Nucleic Acids Res. **18:**1649.
10. **Hanahan, D.** 1983. Studies on transformation of *Escherichia coli* with plasmids. J. Mol. Biol. **166:**557–580.
11. **Johnston, R. F., S. C. Pickett, and D. L. Barker.** 1990. Autoradiography using storage phosphor technology. Electrophoresis **11:**355–360.
12. **Krevolin, M. D., and R. Calendar.** 1985. The replication of bacteriophage P4 DNA *in vitro*: partial purification of the P4 α gene product. J. Mol. Biol. **182:**509–517.
13. **Lanka, E., and P. T. Barth.** 1981. Plasmid RP4 specifies a deoxyribonucleic acid primase involved in its conjugal transfer and maintenance. J. Bacteriol. **148:**769–781.
14. **Lanka, E., E. Scherzinger, E. Günther, and H. Schuster.** 1979. A DNA primase specified by I-like plasmids. Proc. Natl. Acad. Sci. USA **76:**3632–3636.
15. **LaVallie, E. R., E. A. DiBlasio, S. Kovacic, K. L. Grant, P. F. Schendel, and J. M. McCoy.** 1993. A thioredoxin gene fusion expression system that circumvents inclusion body formation in the *E. coli* cytoplasm. Bio/Technology **11:**187–193.
16. **Lindqvist, B. H., G. Dehò, and R. Calendar.** 1993. Mechanisms of genome propagation and helper exploitation by satellite phage P4. Microbiol. Rev. **57:**683–702.
17. **Lindqvist, B. H., and E. W. Six.** 1971. Replication of bacteriophage P4 DNA in a nonlysogentic host. Virology **43:**1–7.
18. **Mendelman, L. V., B. B. Beauchamp, and C. C. Richardson.** 1994. Requirement for a zinc motif for template recognition by the bacteriophage T7 primase. EMBO J. **13:**3909–3916.
19. **Pansegrau, W., D. Balzer, V. Kruft, R. Lurz, and E. Lanka.** 1990. *In vitro* assembly of relaxosomes at the transfer origin of plasmid RP4. Proc. Natl. Acad. Sci. USA **87:**6555–6559.
20. **Pansegrau, W., and E. Lanka.** 1992. A common sequence motif among prokaryotic DNA primases. Nucleic Acids Res. **20:**4931.
21. **Pérez-Martin, J., G. H. del Solar, R. Lurz, A. G. de la Campa, B. Dobrinski, and M. Espinosa.** 1989. Induced bending of plasmid pLS1 DNA by the plasmid-encoded protein RepA. J. Biol. Chem. **264:**21334–21339.
22. **Qian, X., S. N. Gozani, H. Yoon, C. Jeon, K. Agarwal, and M. A. Weiss.** 1993. Novel zinc finger motif in the basal transcriptional machinery: three-dimensional NMR studies of the nucleic acid binding domain of transcriptional elongation factor TFIIS. Biochemistry **32:**9944–9959.
23. **Sambrook, J., E. T. Fritsch, and T. Maniatis.** 1989. Molecular cloning: a laboratory manual. Cold Spring Harbor Laboratory, Cold Spring Harbor, N.Y.
24. **Sanger, F., S. Nicklen, and A. R. Coulson.** 1977. DNA sequencing with chain-terminating inhibitors. Proc. Natl. Acad. Sci. USA **74:**5463–5467.
25. **Sayers, J. R., W. Schmidt, and F. Eckstein.** 1988. 5′→3′ exonucleases in phosphorothioate-based oligonucleotide-directed mutagenesis. Nucleic Acids Res. **16:**791–802.
26. **Stamford, N. P., P. E. Lilley, and N. E. Dixon.** 1992. Enriched sources of *Escherichia coli* replication proteins. The DnaG primase is a zinc metalloprotein. Biochim. Biophys. Acta **1132:**17–25.
27. **Strack, B., M. Lessl, R. Calendar, and E. Lanka.** 1992. A common sequence motif, -E-G-Y-A-T-A-, identified within the primase domains of plasmid-encoded I- and P-type DNA primases and the α protein of the *Escherichia coli* satellite phage P4. J. Biol. Chem. **267:**13062–13072.
28. **Terzano, S., R. Christian, F. H. Espinoza, R. Calendar, G. Dehò, and D. Ghisotti.** 1994. A new gene of bacteriophage P4 that controls DNA replication. J. Bacteriol. **176:**6059–6065.
29. **Zavitz, K. H., and K. J. Marians.** 1993. Helicase-deficient cysteine to glycine substitution mutants of Escherichia coli replication protein PriA retain single-stranded DNA-dependent ATPase activity. Zn^{2+} stimulation of mutant PriA helicase and primosome assembly activities. J. Biol. Chem. **268:**4337–4346.
30. **Ziegelin, G., R. Calendar, D. Ghisotti, S. Terzano, and E. Lanka.** 1997. Cnr protein, the negative regulator of bacteriophage P4 replication, stimulates specific DNA binding of its initiator protein α. J. Bacteriol. **179:**2817–2822.
31. **Ziegelin, G., and E. Lanka.** 1995. Bacteriophage P4 DNA replication. FEMS Microbiol. Rev. **17:**99–107.
32. **Ziegelin, G., N. A. Linderoth, R. Calendar, and E. Lanka.** 1995. Domain structure of phage P4 α protein deduced by mutational analysis. J. Bacteriol. **177:**4333–4341.
33. **Ziegelin, G., E. Scherzinger, R. Lurz, and E. Lanka.** 1993. Phage P4 α protein is multifunctional with origin recognition, helicase and primase activities. EMBO J. **12:**3703–3708.